

Figure S1: **Wind tunnel and flow profile.** (A) Picture of wind tunnel setup. The Eiffel-type wind tunnel used in this experiment is located at Georgia Institute of Technology (Atlanta, GA, USA). It was designed, constructed, and tested by Engineering Laboratory Design, Incorporated (Lake City, MN, USA). It is a low speed, open circuit wind tunnel situated in a room with dimensions 11.3 x 24.88 x 2.96 m (length x width x height). (B) Wind speed measurements v. downstream position with (green) and without (black) the flower present. Measurements were taken at three lateral (x-direction) positions spaced 4 cm apart (shown in Fig. 2A), but only flow along the centerline showed changes due to the flower. Symbols for the flower wake are enlarged for clarity. Downstream positions are: (1) 20 cm downstream of front mesh, (2) 40 cm downstream of front mesh, (3) expected moth position (80 cm downstream), (4) 85 cm downstream of front mesh, (5) 90 cm downstream of front mesh, (6) 110 cm downstream of front mesh, and (7) 130 cm downstream of front mesh (20 cm upstream of back mesh). Without the flower present, the flow speed profile was uniform across the full length of the working section with variation $\pm 0.01 \text{ ms}^{-1}$ (black data points). With the flower, all flow variation occurred downstream, along the centerline (green x-symbol). In this region, flow speed increases from approximately 0.2 ms^{-1} at the expected moth position (approximately 80 cm downstream), to 0.6 ms^{-1} at 110 cm downstream with velocity variation $\pm 0.02 \text{ ms}^{-1}$. At 130 cm downstream wake effects of the flower were dissipated and the flow speed once again matched the 0.7 ms^{-1} free-stream velocity. Flow upstream of the flower was uniform and consistent with velocity measurements made without the flower present.

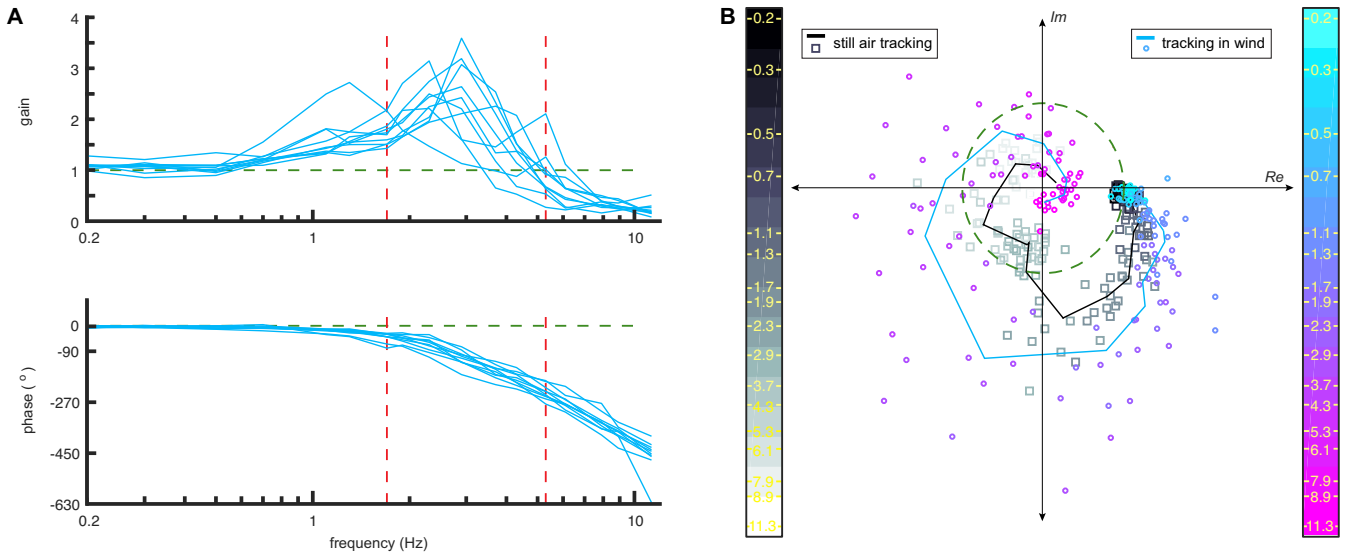


Figure S2: **Individual bode and average complex tracking response with and without wind.** (A) Gain and phase of all 10 individual moths for tracking in wind. The region of vortex shedding frequencies is bounded between 1.7 Hz and 5.3 Hz (red lines). (B) Complex tracking response with and without wind. Perfect tracking corresponds to (1,0) on the green unit circle. Gain and phase are represented in terms of radius and angle around the circle, respectively. Data points correspond to individuals and solid lines represent the mean. Color bars identify how tracking varies across all driving frequencies in still air (greyscale squares) and wind (cool scale, circles). All still air data (black line, greyscale squares) previously collected in Sponberg et al (2015).

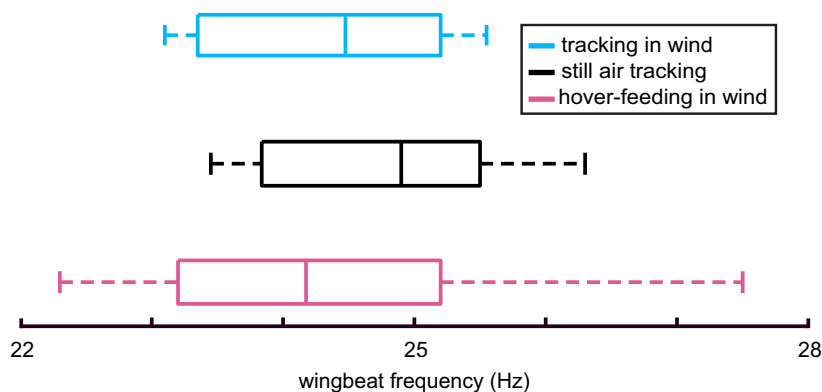


Figure S3: **Wingbeat frequency shows relatively little change across experimental conditions.** Boxplots of wingbeat frequency for tracking in wind (blue), still air tracking (black), and hover-feeding in wind (pink). Median wingbeat frequency varies by less than 1 Hz between the three conditions. Whiskers correspond to the most extreme data points and the boundaries of the box denote the 25th and 75th data percentiles.

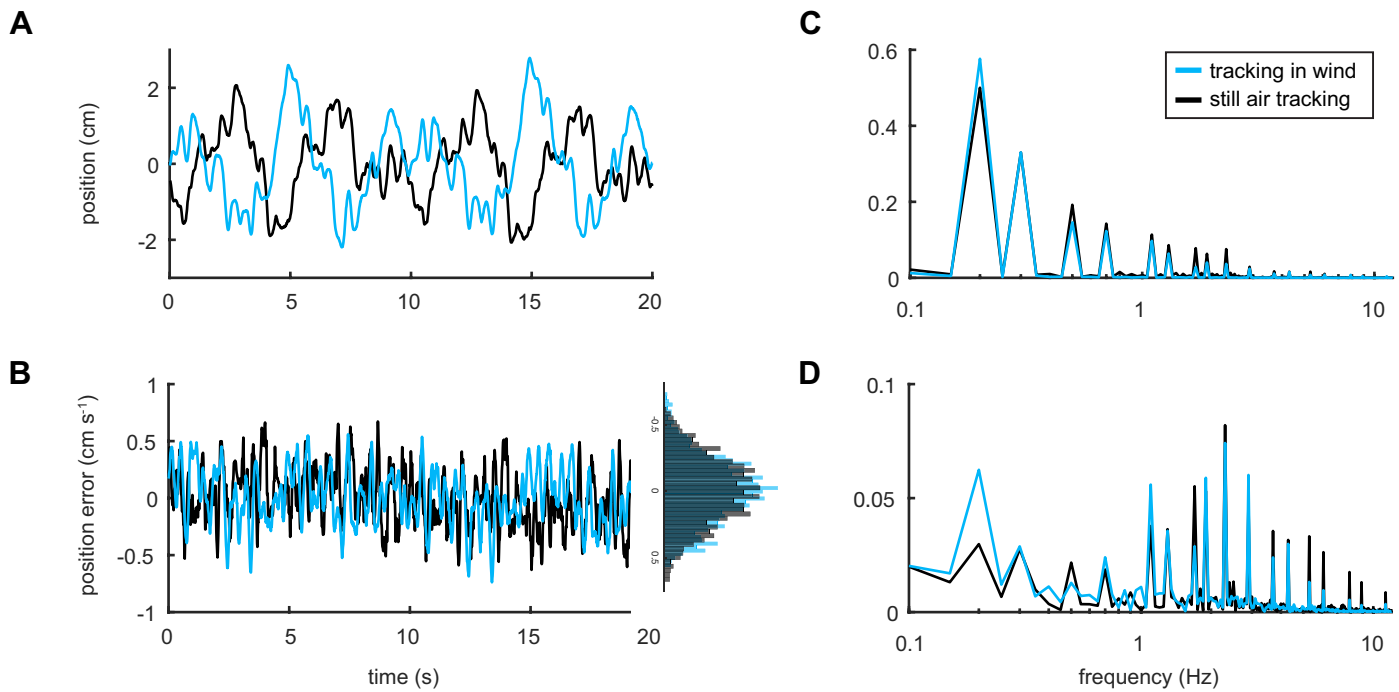


Figure S4: **Position error in the flower wake.** All still air data (black) previously collected in Sponberg et al (2015). (A) Averaged time series data for tracking with and without wind. (B) Position error with and without wind. Differences in the time traces are emphasized with the inset histogram. In wind, position error increases and moths spend more time further from the flower. (C) Amplitude (position) in the frequency domain (after Fourier transform of data from A). Peaks correspond to prescribed flower driving frequencies. (D) Position error in the frequency domain (after Fourier transform of data from B). Tracking is dominated by low frequency oscillations due to the stimulus design. In wind, position error increases across low frequencies, but decreases at high frequencies. Across all frequencies tracking performance is decreased and higher frequency oscillations are removed.

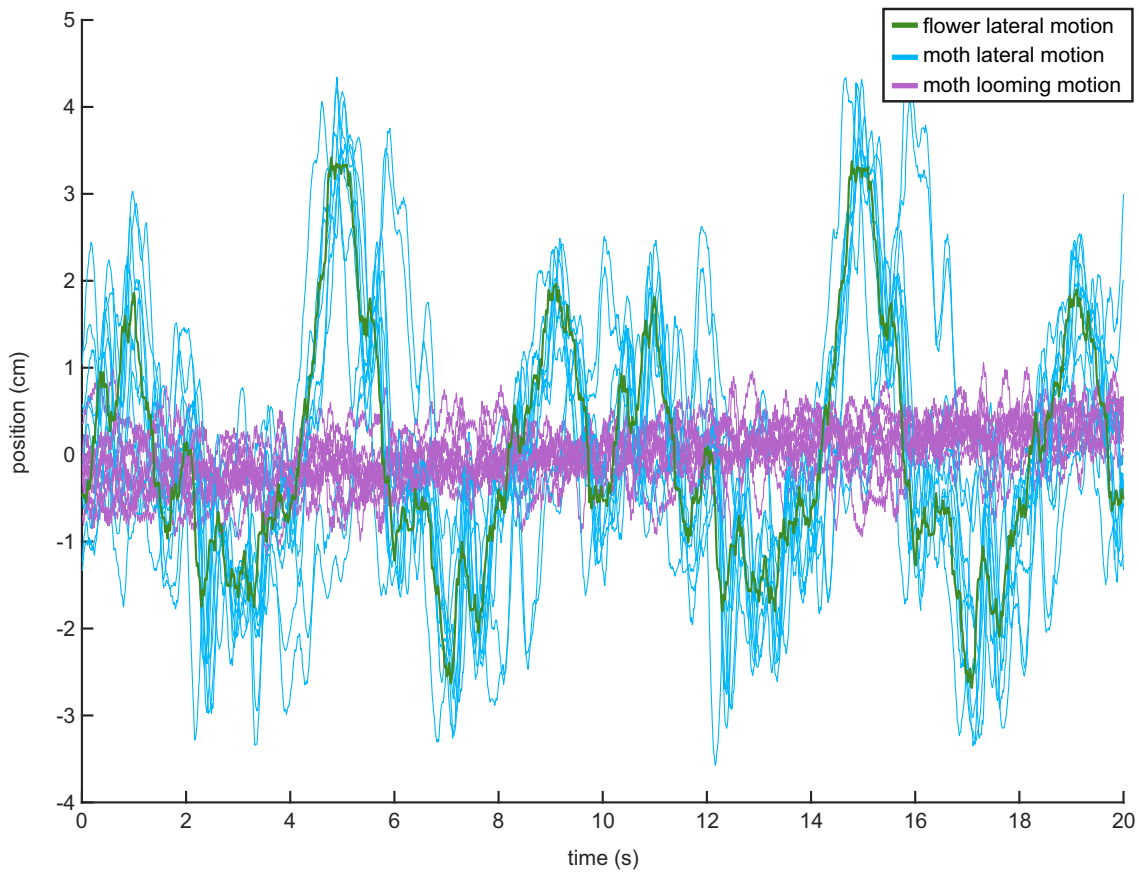


Figure S5: **Lateral oscillations dominate tracking motion.** Raw time series data for individual trials of tracking in wind. The flower motion (green) is bounded between ± 3 cm in the x-direction, but the moth (blue) overshoots the flower sometimes reaching 4 cm lateral displacements. Off-axis oscillations in the looming, or y-direction, are small compared to lateral motion. Moths maintain position ± 1 cm downstream of the flower.



Movie 1. **Smoke visualization video of the robotic flower wake.** Smoke plane is aligned with the center of the flower and playback is at 30 fps (recorded at 125 fps). Vortices in the flower wake are shed within the frequency range 2-5 Hz. The flower wake is best described by a range of frequencies due to the complex shape of the flower face and nectary combined. Global level and contrast adjustments were performed in iMovie to better visualize the smoke lines.



Movie 2. **Smoke visualization video of the leading-edge vortex (LEV) at mid-wing.** Smoke plane is aligned with mid-wing on the moth (approximately 3-4 cm off center) and playback is at 30 fps (recorded at 125 fps). Although the wings are interacting with vortices shed off of the flower, the LEV remains bound to the wing throughout the downstroke and is best seen during mid-downstroke. Global level and contrast adjustments were performed in iMovie to better visualize the smoke lines.



Movie 3. **Smoke visualization video of the leading-edge vortex (LEV) over the tho-rax.** Smoke plane is aligned with the center of the flower and playback is at 30 fps (recorded at 125 fps). Although the wings are interacting with vortices shed off of the flower, the LEV remains bound to the wing throughout the downstroke and is best seen during mid-downstroke. Global level and contrast adjustments were performed in iMovie to better visualize the smoke lines.